

- (4) H. R. Allcock, *Angew. Chem., Int. Ed. Engl.*, **16**, 147 (1977).
- (5) N. S. Schneider, C. R. Desper, and R. E. Singler, *J. Appl. Polym. Sci.*, **20**, 3087 (1976).
- (6) C. R. Desper and N. S. Schneider, *Macromolecules*, **9**, 424 (1976).
- (7) C. R. Desper, N. S. Schneider, and E. Higginbotham, *J. Polym. Sci., Polym. Lett. Ed.*, **15**, 457 (1977).
- (8) M. N. Alexander, C. R. Desper, P. L. Sagalyn, and N. S. Schneider, *Macromolecules*, **10**, 721 (1977).
- (9) N. S. Schneider, C. R. Desper, and J. J. Beres, "Liquid Crystalline Order in Polymers", A. Blumstein, Ed., Academic Press, New York, 1978, p 299.
- (10) N. S. Schneider, C. R. Desper, R. E. Singler, M. N. Alexander, and P. L. Sagalyn, "Advances in Organometallic Polymers", C. E. Carraher and J. E. Sheats, Eds., Academic Press, New York, 1978, p 271.
- (11) S. H. Rose, *J. Polym. Sci., Polym. Lett. Ed.*, **6**, 837 (1968).
- (12) D. P. Tate, *Rubber World*, **172**, 41 (1975).
- (13) J. E. Thompson and K. A. Reynard, *J. Appl. Polym. Sci.*, **21**, 2575 (1977).
- (14) E. J. Quinn and R. L. Dieck, *J. Cell Plast.*, **13**, 96 (1977).
- (15) R. L. Dieck and L. Goldfarb, *J. Polym. Sci., Polym. Chem. Ed.*, **15**, 361, (1977).
- (16) T. M. Connelly, Jr., and J. K. Gillham, *J. Appl. Polym. Sci.*, **20**, 473 (1976).
- (17) R. E. Singler, G. L. Hagnauer, N. S. Schneider, B. R. LaLiberte, R. E. Sacher, and R. W. Matton, *J. Polym. Sci., Polym. Chem. Ed.*, **12**, 433 (1974).
- (18) R. E. Singler and G. L. Hagnauer, "Advances in Organometallic Polymers", C. E. Carraher and J. E. Sheats, Eds., Academic Press, New York 1978, p 257.
- (19) E. G. Stroh, Jr., Ph.D. Thesis, Department of Chemistry, the Pennsylvania State University, 1972.
- (20) S. M. Bishop and I. H. Hall, *Br. Polym. J.*, **6**, 183 (1974).
- (21) B. Wunderlich, "Macromolecular Physics", Vol. 1, Academic Press, New York, 1973, p 147-177.
- (22) G. Natta, P. Corradini, D. Sianesi, and D. Morero, *J. Polym. Sci.*, **51**, 527 (1961).
- (23) R. E. Singler, J. E. White, and S. A. Leone, unpublished results.

Application of the Virtual Bond Method to the Crystalline Conformations of Isotactic Polystyrene and Poly(methyl methacrylate)

P. R. Sundararajan

Xerox Research Centre of Canada, 2480 Dunwin Drive, Mississauga, Ontario L5L 1J9, Canada. Received March 5, 1979

ABSTRACT: The application of the virtual bond method of analysis to the crystalline conformations of vinyl polymers is discussed. The method can be used if the screw symmetry and the pitch of the helix are known from diffraction data and involves the rotation of the repeat unit about its end-to-end vector or the virtual bond. It enables the determination of the favorable conformations of the helix, by allowing the variation of the skeletal bond angle at the methylene carbon atom. The crystalline conformations of isotactic polystyrene with 12 repeat units per turn and 3 repeat units per turn are discussed. The analysis is restricted to showing that the 12-unit helix is stereochemically possible. Rigorous comparison with the X-ray data is not attempted due to the possible presence of head-to-head sequences in the polymer and its influence on the crystalline domains. The calculations on the five-unit helix of isotactic PMMA show that it occurs close to an unfavorable minimum on the (ϕ_i, ϕ_{i+1}) surface. The calculated energy of the ten-unit helix is lower than that of the five-unit helix of PMMA. The side group rotations play an important role in determining the relative positions of these helical conformations on the overall (ϕ_i, ϕ_{i+1}) domain.

Conformational analysis in terms of the rotations around the skeletal bonds has been used to understand the conformational features of several vinyl polymers.¹⁻⁸ Empirical energies of interaction between nonbonded atoms and groups, evaluated for each of the conformations of the dyad, generated by rotations ϕ_i and ϕ_{i+1} as in Figure 1, have been used to calculate the statistical weight parameters and to estimate the unperturbed statistically averaged properties.

The recent work on PMMA⁴ and poly(α -methylstyrene)⁷ showed that a large value of 122-124° is preferred for the skeletal bond angle C ^{α} -C-C ^{α} (denoted by θ''). Crystallographic results⁹ on small molecular analogues support this conclusion. The large deviation from tetrahedral value is due to the bulkiness of the side groups. Similar enlargement of the angle at the bridge atom between repeating units, depending on the size of the substituents, has been observed frequently in di- and polysaccharides.¹⁰ Thus, values of angles greater than 109.5° may have to be used in the calculations depending on the size of the side groups and the intensity of the interaction between them. The energy map, as a function of ϕ_i and ϕ_{i+1} , must therefore be constructed for a range of values of θ'' in assessing the relative stabilities of the conformations and choosing the most preferred conformation. This may not be crucial while calculating the solution properties of these

chains, since the range of angles can be substituted by the most probable average value. However, it becomes important when dealing with the crystalline conformations of vinyl chains and in the refinement of crystal structures.

The (ϕ_i, ϕ_{i+1}) map of the energies shows the overall conformational space available to the dyad of the polymer and is useful in calculating the average properties. However, this may be unnecessary when the analysis of a unique crystalline conformation is desired. This is readily accomplished by using the "virtual bond method", which eliminates the need to construct several ϕ_i, ϕ_{i+1} maps for a range of values of θ'' . The virtual bond method has been effective in predicting the crystalline conformations of several polysaccharides and copolysaccharides.¹¹⁻¹⁴ Its application to polypeptides has been briefly discussed before.¹¹ This method is applicable when the helix parameters are known from diffraction data.

The parameters defining the helical conformation, namely, n , h , $\Delta(360/n)$, and P (repeat distance), can be derived from fiber diffraction data. For the application of the virtual bond method, for a given type of helix, only the monomer geometry is required. The values of θ'' (C ^{α} -C-C ^{α}), ϕ_i , and ϕ_{i+1} are not required, as in other methods; rather, the preferred values of θ'' , ϕ_i , and ϕ_{i+1} are obtained as a *result* of the analysis.¹¹ As shown in Figure 2, the virtual bond is the end-to-end vector of the monomer

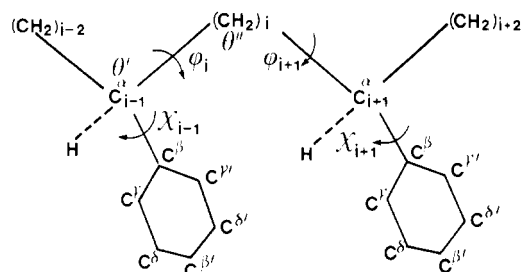


Figure 1. Schematic representation of a segment of isotactic polystyrene. The rotations about the skeletal bonds and the $C^\alpha-C^\beta$ bonds are shown.

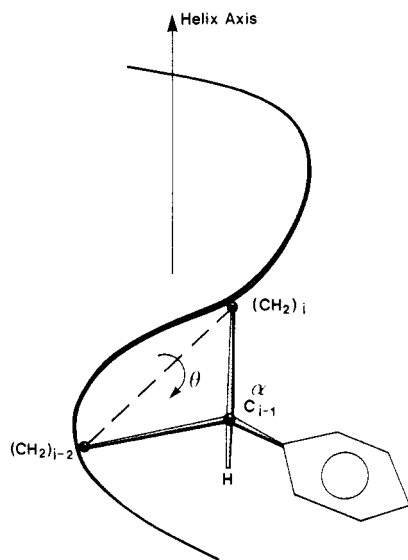


Figure 2. Schematic representation of the virtual bond method. The rotation θ about the virtual bond is shown.

unit, joining successive methylene carbon atoms, in the case of a vinyl chain. This vector may alternatively be chosen with respect to the successive C^α atoms. However, since (i) the bond angle at the C^α atom is close to 110° and the angle at CH_2 is variable over a wider range, and (ii) the ϕ_i and ϕ_{i+1} rotations are centered at CH_2 , it is preferable to choose the virtual bond with respect to the methylene carbons. For a helix of defined n and h , the inclination of the virtual bond with respect to the helix axis is fixed and is readily given by

$$\mu = \cos^{-1}(h/L) \quad (1)$$

where L is the length of the virtual bond. However, the disposition of the other atoms of the repeat unit with respect to the helix axis is as yet undetermined. The rotation θ of the residue, as in Figure 2, about the virtual bond, varies the positions of the atoms of the residue with respect to the helix axis.

After the repeat unit has been transformed to the proper orientation for a value of θ , the contiguous residue can be generated simply by the helix symmetry operation: rotation about the helix axis through $\pm\Delta$ and translation through h along the helix axis. Inter-unit atomic interactions between contiguous repeat units can then be calculated, and the best value of θ defining the helix may be chosen. When the value of θ is changed, the angle θ'' varies. From the coordinates of the contiguous units generated above, θ'' as well as ϕ_i and ϕ_{i+1} can be evaluated. Thus, the values of θ'' , ϕ_i , and ϕ_{i+1} are deduced as a result of the virtual bond method of analysis. The coordinates of the atoms of the helix, for a chosen value of θ , can be directly fed into subroutines for the calculation of Fourier transform or packing of the chains in the lattice. The

mathematics of the method is simple, and the calculations are rapid.

The occurrence of isotactic polystyrene with the threefold helical conformation, with a repeat distance of 6.65 Å, is well known.¹⁵ Recently, Atkins et al.¹⁶ found that the oriented gels of isotactic polystyrene, prepared with *trans*-decalin, exhibited an X-ray pattern, with a periodicity of 30.6 Å along the chain direction, with 24 C-C bonds per turn of the helix. This would lead to 12 monomers per turn of the helix. A meridional reflection at 5.1 Å showed the presence of a sixfold screw axis. This leads to the conclusion that contiguous monomers in a dyad differ in details, such as the pendant group rotation, thus making the dyad, rather than a monomer, the repeating unit. In any case, 12 monomers are required to complete a turn of the helix. This would result in a conformation which is close to the *tt* state of the contiguous bonds of the chain. Assuming that the *tt* state is inadmissible for isotactic vinyl chains, Atkins et al. took their sample to consist of syncephalic (a term used by these authors to define head-to-head, tail-to-tail sequences) stereosequence, in order to account for the repeat of 30.6 Å. The ¹³C NMR data of the sample however showed that the polymer was isotactic, to the extent of 98%. Thus, the contradiction between their NMR data and their proposed syncephalic sequence is mainly due to their assumption that the *tt* state is unfavorable for isotactic vinyl chains.¹⁷ Most importantly, the experimental confirmation that the extended conformation reverts to the conventional three-fold helical structure upon heating the gel assures that the polymer is isotactic with head-to-tail sequences, and syncephalic sequences, if any, would be of very low incidence.

Consider a vinyl chain in which the skeletal bond angle at the C^α atom is taken to be 110° , and the angle at the methylene carbon atom is taken to be 120° . Due to the inequality of 10° in the bond angles, an all-*trans* chain, with $\phi_i = \phi_{i+1} = 0^\circ$, would not have a rectilinear axis but would close upon itself after 36 units ($360/10$). A rotation of about 20° in ϕ_i and ϕ_{i+1} not only relieves the $R_{i-1}-R_{i+1}$ interaction but also prevents the chain closure, rendering a worm-like helical character to the chain, with a large repeat distance. It is shown here, using the virtual bond method, that such an extended chain is stereochemically possible for isotactic polystyrene and occurs close to the minimum energy position on the (ϕ_i, ϕ_{i+1}) surface. Rigorous attempts at refining the conformation to account for all the details of the X-ray pattern are not made here.

A fivefold helical conformation, with a repeat distance of 10.4 Å, was proposed for isotactic PMMA by Liquori et al.¹⁸ Recently, Tadokoro and co-workers¹⁹ re-examined the X-ray data and derived a double-helical structure for isotactic PMMA. Each strand of the double helix consists of ten repeat units per turn, with a repeat distance of 20.8 Å. According to these authors,¹⁹ the presence of a twofold axis between the strands essentially halves this repeat distance, and the X-ray pattern shows a repeat of 10.4 Å. The exact nature of the structure of isotactic PMMA still remains in doubt. The virtual bond method is applied to both 5(2.08) and 10(2.08) helices²⁰ to derive their conformational features.

Crystalline Conformations of Isotactic Polystyrene

Parameters for the Calculations. The geometry of the repeat unit, shown in Figure 2, was chosen with the bond lengths and bond angles used previously,⁵ with the exception of the angle $CC^\alpha C$. A value of 109.5° was used for this angle, unless specified otherwise. The nonbonded

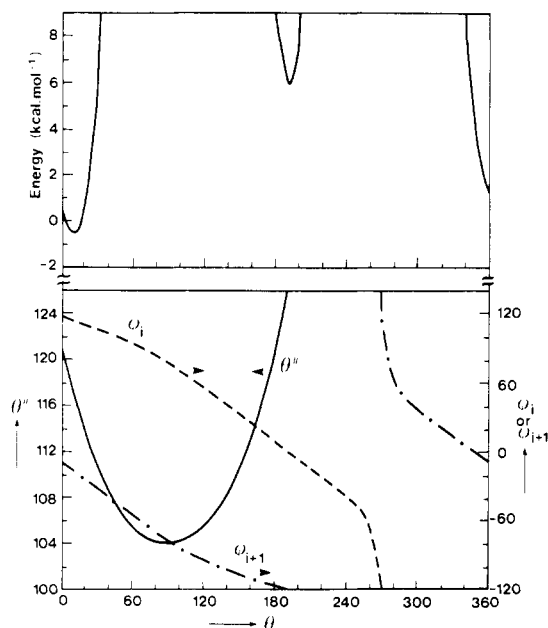


Figure 3. Results of the virtual bond analysis for the right-handed 3(2.216) helix. The values of θ'' (left ordinate) and ϕ_i and ϕ_{i+1} (right ordinate) are plotted with respect to the virtual bond rotation angle θ , in the lower part. The energy curve is given in the upper part.

and torsional energies were calculated following Yoon et al.⁵ The van der Waals radii were chosen to be 0.1 Å shorter than the previous values used for the calculation of solution properties. The energy due to the deviation of the skeletal valence angle from 109.5° was calculated using the expression given before.⁴ The signs of the rotations ϕ_i and ϕ_{i+1} were taken to be consistent with the nomenclature of Flory et al.²¹

Threefold Polystyrene Helix. The work of Natta et al.¹⁵ showed that isotactic polystyrene crystallizes with three repeat units in a repeat distance of 6.65 Å. Figure 3 shows the results of the virtual bond analysis for the right-handed 3(2.216) helix. The values of θ'' , ϕ_i , and ϕ_{i+1} have been plotted as a function of θ , in the lower part of the figure, and the energy curve is given in the upper part. It is seen that the angle θ'' varies from 104 to 125°, as θ is varied from 0 to 190°. Except at the minimum of the θ'' curve, two values of θ give rise to the same value of θ'' . For example, $\theta = 22$ and 153° correspond to $\theta'' = 112^\circ$. This means that for any given value of θ'' (except at the minimum of the θ'' curve) two right-handed helices are possible. The values of ϕ_i and ϕ_{i+1} for a chosen value of θ'' can be determined from this figure. This is done simply by determining the ϕ_i and ϕ_{i+1} corresponding to the values of θ , which yield the chosen value of θ'' . For example, for $\theta'' = 112^\circ$, the 3(2.216) helix is possible with $(\phi_i, \phi_{i+1}) = (110^\circ, -23^\circ)$ and $(23^\circ, -110^\circ)$. The minimum in the θ'' curve corresponds to a value of 104°. This implies that when $\theta' = 109.5^\circ$ and $\theta'' = 104^\circ$, only one right-handed helix can be constructed, with $(\phi_i, \phi_{i+1}) = (79^\circ, -79^\circ)$. For values of $\theta'' < 104^\circ$, it would be impossible to construct a 3(2.216) helix, with the chosen θ' and skeletal bond lengths.

Figure 3 shows that the energy of interaction is favorable only over a narrow range of the virtual bond rotation angle θ . The minimum in energy occurs at $\theta = 10^\circ$, which corresponds to $\theta'' = 117^\circ$, $\phi_i = 113^\circ$, and $\phi_{i+1} = -16^\circ$. This value of 117° for θ'' is larger than the value of 114° hitherto used in the conformational analysis of PS and derivatives. The value of 114° occurs at $\theta = 20^\circ$. If nonbonded interactions alone are considered, the energies corresponding to $\theta'' = 117$ and 114° are -2.4 and -0.5 kcal mol⁻¹, re-

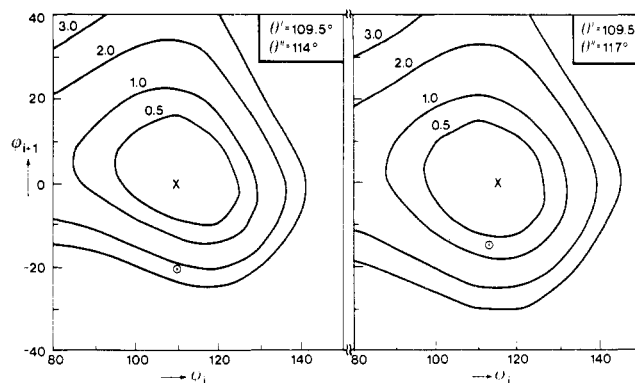


Figure 4. Energy contours for a meso dyad of polystyrene in terms of ϕ_i and ϕ_{i+1} are shown for $\theta' = 109.5^\circ$, $\theta'' = 114^\circ$ (left), and $\theta'' = 117^\circ$ (right). Contours are drawn, in kcal mol⁻¹ at intervals of energy marked on the curves, with respect to the minima marked by X. The positions of the 3(2.216) helix are marked by O.

spectively. This is not surprising since an increase in θ'' increases the distance between the interacting groups, and the energy is reduced. However, the value of 117° is preferred over 114°, by about 1.6 kcal mol⁻¹, even if the energy due to bond angle deformation is included. Varying the side group rotation angle χ in the range of $\pm 20^\circ$ did not change the position, energy value, or the shape of the minima. Although the 3(2.216) helix is possible with $\theta'' = 117^\circ$ when $\theta = 170^\circ$, the values of ϕ_i and ϕ_{i+1} are 16 and -113°, respectively. This conformation is of very high energy since ϕ_{i+1} corresponds to the \bar{g} state and thus entails severe steric interactions as noted before.⁵

Figure 4 shows the energy maps in terms of ϕ_i and ϕ_{i+1} , using $\theta' = 109.5^\circ$, $\theta'' = 114^\circ$ and $\theta' = 109.5^\circ$, $\theta'' = 117^\circ$. Energy contours, with values marked, were drawn with respect to the minimum energy in each case. The positions of the 3(2.216) helix for $\theta'' = 114$ and 117° are marked in the respective map. It is seen that with $\theta'' = 114^\circ$, the 3(2.216) conformation occurs outside of the contour for 2 kcal mol⁻¹. It is higher than the minimum energy by about 2.3 kcal mol⁻¹. However, with $\theta'' = 117^\circ$, the 3(2.216) position is just outside the contour for 0.5 kcal mol⁻¹. Thus, in terms of the overall (ϕ_i, ϕ_{i+1}) domain of the chain, the 3(2.216) helix with $\theta'' = 117^\circ$ is closer to the minimum energy position.

Extended Conformation of Isotactic Polystyrene

The X-ray pattern of oriented gels of isotactic polystyrene¹⁶ showed that 12 monomers (24 C-C bonds) are contained in a repeat distance of 30.6 Å. Although slight differences between contiguous units may reduce the 12-fold symmetry to 6-fold,¹⁶ the stereochemical feasibility of the helix with 12 repeat units is a prerequisite, and this feature is examined here. The calculations were performed using $n = 12$ and $h = 2.55$ Å. Perturbations may then be introduced in terms of unequal side group rotations, etc., to account for the details of the X-ray pattern.

In this case also, the virtual bond was chosen so as to span the successive methylene carbons. With $\theta' = 110^\circ$, the length of the virtual bond is less than 2.55 Å. Hence, a value of 114° was taken, so that with a C-C bond length of 1.53 Å the length of the virtual bond becomes 2.566 Å. The results of the analysis are shown in Figure 5. The values of θ'' , ϕ_i , and ϕ_{i+1} are given in the lower part of the figure. It is seen that unlike the situation in Figure 3, θ'' varies only from 113.2 to 119.8°, as the value of θ ranges from 0 to 360°. The values of ϕ_i are positive and those of ϕ_{i+1} negative throughout this range. For any value of θ'' , two right-handed helices are possible. For example, with

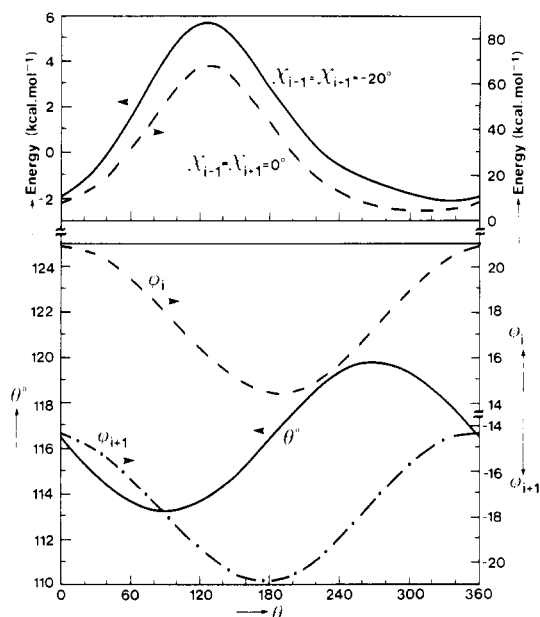


Figure 5. Results of the virtual bond analysis for the right-handed 12(2.55) helix. The values of θ'' , ϕ_i , and ϕ_{i+1} as a function of θ are given in the lower part (see legend to Figure 3). The energy curves are shown in the upper part for two values of side group rotation angles.

$\theta'' = 114^\circ$, the right-handed 12(2.55) helix occurs with $(\phi_i, \phi_{i+1}) = (19.9^\circ, -15.8^\circ)$ and $(15.8^\circ, -19.9^\circ)$. The θ'' curve shows a maximum at 119.8° and a minimum at 113.2° . This means that a 12(2.55) helix cannot be constructed if θ'' is less than 113.2° or greater than 119.8° .

The upper part of Figure 5 shows the energy curve for the side group rotations $(\chi_{i-1}, \chi_{i+1}) = (0^\circ, 0^\circ)$ (right ordinate) and $(-20^\circ, -20^\circ)$ (left ordinate). With both sets of side group rotations, the energy curve shows a maximum in the range of $\theta = 120$ – 130° , corresponding to $\theta'' = 113.6$ – 114° . Both curves show the minimum energy in the range of $\theta = 240$ to 360° . With $\chi_{i-1} = \chi_{i+1} = 0^\circ$, the minimum in energy occurs at $\theta = 315^\circ$, with an energy of $4.5 \text{ kcal mol}^{-1}$. This corresponds to a conformation with $\theta'' = 118.8^\circ$ and $(\phi_i, \phi_{i+1}) = (19.7^\circ, -15.1^\circ)$. However, with $\chi_{i-1} = \chi_{i+1} = -20^\circ$, the energy at the minimum decreases to $-2.1 \text{ kcal mol}^{-1}$, for the value of $\theta = 335^\circ$. This conformation is defined by $\theta'' = 117.8^\circ$ and $(\phi_i, \phi_{i+1}) = (20.4^\circ, -14.5^\circ)$. For $\chi_{i-1} = \chi_{i+1} = 0^\circ$, the significant overlaps are due to the pairs $C^{\beta}_{i-1}-C^{\nu}_{i+1}$ (2.78 Å), $C^{\nu}_{i-1}-C^{\beta}_{i+1}$ (2.98 Å), $C^{\nu}_{i-1}-C^{\nu}_{i+1}$ (2.88 Å), and $C^{\delta}_{i-1}-C^{\delta}_{i+1}$ (2.82 Å). With $\chi_{i-1} = \chi_{i+1} = -20^\circ$, the distances between these pairs of atoms increase to 3.18, 3.35, 3.63, and 3.63 Å, respectively, thus reducing the energy. Larger rotations, e.g., $(-30, -30)$, decrease the energy insignificantly, and the location of the minimum energy is unaffected. Side group rotations of the type $(\chi_{i-1}, \chi_{i+1}) = (20, 20)$, $(20, -20)$, and $(-20, 20)$ are not favorable since these rotations decrease the distances between the atoms of adjacent phenyl groups.

The value of $\theta'' = 117.8^\circ$ is possible for $\theta = 205^\circ$ as well. Here, $(\phi_i, \phi_{i+1}) = (14.5^\circ, -20.4^\circ)$. This conformation is about 3 kcal mol^{-1} higher in energy than the conformation corresponding to $\theta = 335^\circ$ when $\chi_{i-1} = \chi_{i+1} = -20^\circ$. The distances $C^{\beta}_{i-1}-C^{\nu}_{i+1}$ (3.0 Å) and $C^{\nu}_{i-1}-C^{\nu}_{i+1}$ (2.86 Å) with $\theta = 205^\circ$ are increased to 3.2 and 3.1 Å, respectively, in the conformation with $\theta = 335^\circ$.

Figure 6 shows the energy maps in terms of ϕ_i and ϕ_{i+1} , calculated for $\theta' = 114^\circ$ and $\theta'' = 117.8^\circ$, with $\chi_{i-1} = \chi_{i+1} = 0$ and -20° . The position of the 12(2.55) helix is also marked on these maps. It is seen that with $\chi_{i-1} = \chi_{i+1} = 0^\circ$, the minimum in energy occurs at $(\phi_i, \phi_{i+1}) = (15^\circ, 15^\circ)$.

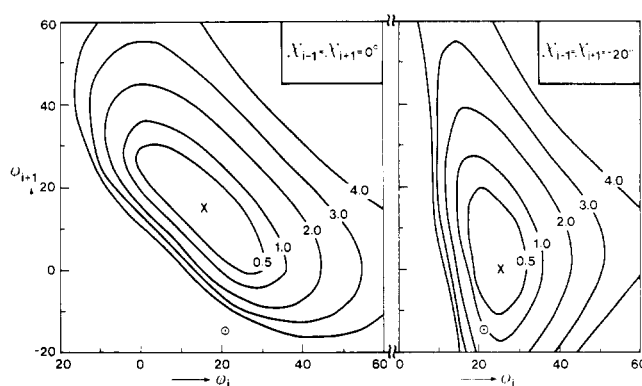


Figure 6. Energy maps for a meso dyad of polystyrene, in terms of ϕ_i and ϕ_{i+1} , are shown for two sets of side group rotation angles. Contours are in kcal mol^{-1} , at intervals of energy marked on the curves, with respect to the minima marked by \times . The positions of the 12(2.55) helix are marked by \circ . $\theta' = 114^\circ$; $\theta'' = 117.8^\circ$.

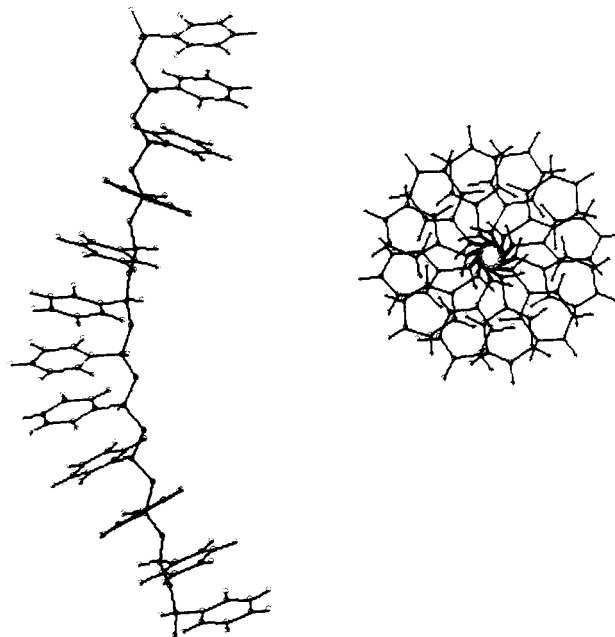


Figure 7. Projections of the 12(2.55) helical conformation, parallel to and normal to the helix axis.

The 12(2.55) conformation, with $(\phi_i, \phi_{i+1}) = (20.4, -14.5)$, is far removed from the minimum energy position and is about $9.5 \text{ kcal mol}^{-1}$ higher in energy. However, with $\chi_{i-1} = \chi_{i+1} = -20^\circ$, the minimum energy position is shifted to $(25^\circ, 0^\circ)$, and the energy of the 12(2.55) conformation is only about $1.0 \text{ kcal mol}^{-1}$ higher than the minimum in the overall (ϕ_i, ϕ_{i+1}) surface of the dyad. Thus, it is shown that the extended conformation with $n = 12$ and $h = 2.55 \text{ Å}$ is stereochemically possible for isotactic polystyrene. Comparison of the energies at the minima in Figures 3 and 5 shows that the 12(2.55) helix is of lower energy than the 3(2.216) helix. The projections of the 12(2.55) helix are shown in Figure 7.

Fourier transforms calculated with the 12(2.55) helix failed to account for the general features of the X-ray pattern. The latter showed greater intensities on the even-order layer lines than on the odd-order layers and a meridional reflection on the sixth layer line. If a small inequality is introduced in the side group rotation angles, e.g., with $\chi_{i-1} = -20^\circ$ and $\chi_{i+1} = -30^\circ$, the dyad has to be considered as the repeat unit. In such a case, 12-fold symmetry is reduced to 6-fold, and $n = 6$ and $h = 5.1 \text{ Å}$. Calculations with such a conformation reproduced the meridional reflection on the sixth layer line, and although

the calculated intensities of the even-order layer lines were somewhat stronger than the odd-order layers, the intensity of the first layer was as strong as the second.

The possibility of using the dyad unit, with various sets of ϕ_i and ϕ_{i+1} , was then examined. That is, the conformation of the repeat unit itself was treated as a variable. None of the accessible conformations of ϕ_i and ϕ_{i+1} had an end-to-end distance of greater than 5.1 Å by using $\theta' = 109.5^\circ$ and $\theta'' = 114^\circ$. Hence, the dyad with $\theta' = 114^\circ$ and $\theta'' = 117.8^\circ$ was chosen. The dyad was generated for a particular value of ϕ_i and ϕ_{i+1} , and this conformation was used for the virtual bond analysis, for $n = 6$ and $h = 5.1$ Å. Even in such an analysis, the first layer line was calculated to be as strong as the second layer line. Otherwise, the Fourier transform calculations were satisfactory.

It would thus seem that consideration of a single helical chain is not sufficient to reproduce the finer details of the X-ray pattern. Since the experimental sample was a gel, the possibility of multiple helices exists. Preliminary calculations show that a double helix, with a twofold axis or a twofold screw axis between the chains, is stereochemically possible. Each strand would then be a 12(2.55) helix, and the minimum distance between the axes of the two 12(2.55) helices should be about 6 Å. Atkins et al.¹⁶ also observed that the 12(2.55) and the 3(2.216) helices exist simultaneously when the sample was dried or annealed at 95 °C, and the conversion 12(2.55) \rightarrow 3(2.216) was complete at 150 °C. This would mean that the solvent molecules might play a role in stabilizing the 12(2.55) helical structure. Thus, any attempt at calculating the X-ray intensities should include bound solvent molecules as well. Exhaustive calculations on the mode of interaction between the helices and the solvent molecules, the multiple helices, etc., are thus clearly indicated.

Crystalline Conformations of Isotactic PMMA

Five-Residue Helix. The structure proposed by Li-quori and co-workers¹⁸ for isotactic PMMA consists of a helical conformation with five repeat units per turn, with a repeat distance of 10.4 Å. The results of the virtual bond analysis of the right-handed 5(2.08) helix are shown in Figure 8. A restricted range of θ is presented here. The geometrical parameters and the energy functions and parameters are the same as those used previously⁴ except that the van der Waals radii were taken to be 0.1 Å shorter. It is seen that within the ranges of $\theta = 180$ –220 and 320–360°, the value of θ'' varies from 110 to 128°. The variations of ϕ_i and ϕ_{i+1} are very small in this region. As in the case of polystyrene, two right-handed helices are possible for any value of θ'' shown in Figure 8. For example, with $\theta'' = 120^\circ$, the two 5(2.08) helices correspond to $(\phi_i, \phi_{i+1}) = (-4^\circ, -73^\circ)$ and $(73^\circ, 4^\circ)$. The value of $\pm 73^\circ$ for one of the skeletal bond rotations is close to the eclipsed conformation of the skeletal bonds. Within the range of θ shown in Figure 8, this angle varies only from 71.4 to 73.3°. This is reminiscent of the minima calculated by Suter and Flory,²² at $(\phi_i, \phi_{i+1}) \approx (10^\circ, 50^\circ)$, $(50^\circ, 10^\circ)$, $(70^\circ, 110^\circ)$, and $(110^\circ, 70^\circ)$ for the meso dyad of polypropylene. The formation of a stable crystalline form with such a near-eclipsed conformation of the bonds would require distortion of the side groups from the preferred conformations usually assigned to them with respect to the skeletal bonds.²³

The energies of the conformations of the 5(2.08) helix are shown in the upper part of Figure 8. The solid curve corresponds to $\chi_{i-1} = \chi_{i+1} = 0^\circ$, in which the C=O bond eclipses the C-CH₃ bond. The minimum in the energy curve occurs in the range of $\theta = 335$ –340°, which corre-

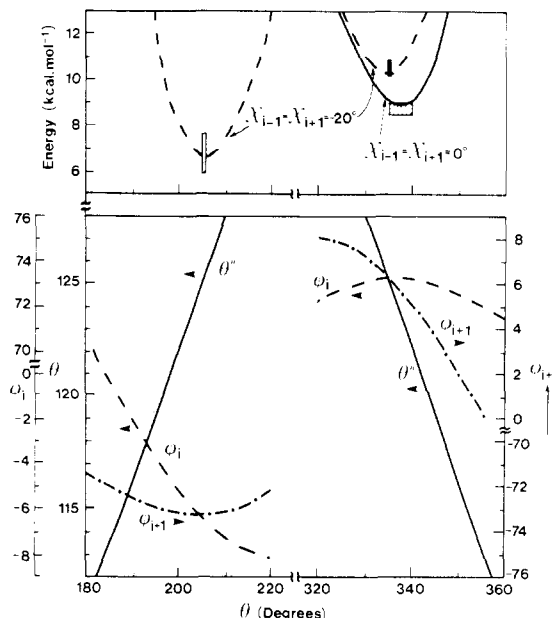


Figure 8. Results of the virtual bond analysis for the right-handed 5(2.08) helix of PMMA. See legend to Figure 3. The energy curves are given for two sets of side group rotation angles. The dotted area denotes the minimum energies when χ_{i-1} and χ_{i+1} are -20 or 160° ; the shaded area, when $\chi_{i-1} = \pm 20$ or ± 160 and $\chi_{i+1} = -20$ or 160 ; and the cross-hatched area, when $\chi_{i-1} = 0, \pm 20$ or $\pm 160^\circ$ and $\chi_{i+1} = 0, 20$, or -160° .

sponds to $\theta'' = 125.1$ – 122° , and $(\phi_i, \phi_{i+1}) \approx (73.3^\circ, 6.3^\circ)$. The other conformation with $\theta'' = 125^\circ$, occurring at $\theta = 205^\circ$, is of very high energy. However, if $\chi_{i-1} = \chi_{i+1} = -20^\circ$, a minimum occurs at $\theta = 205^\circ$, which is less in energy than the minimum at $\theta = 335^\circ$, as shown by the broken curve. Various combinations of χ_{i-1} and χ_{i+1} , with $0^\circ, \pm 20^\circ, 180^\circ$, and $\pm 160^\circ$, were used. The shaded, cross-hatched, and dotted areas in the energy diagram show the range of energy values at the minima. The minimum corresponding to $\theta = 205^\circ$ occurs only if $(\chi_{i-1}, \chi_{i+1}) = (-20^\circ, -20^\circ)$, $(-20^\circ, 160^\circ)$, $(160^\circ, -20^\circ)$ or $(160^\circ, 160^\circ)$. The energy is very high for all the other combinations of rotations.

The minimum at $\theta = 335^\circ$ is less sensitive to the variations in χ . The minima are restricted to the range of energy values indicated by the boxed areas. In this conformation, the value of $\phi_i = 73^\circ$, and hence the interaction of $(\text{COOCH}_3)_{i-1}$ with the other groups, is negligible. The energy then depends mainly on the values of χ_{i+1} . The shaded area corresponds to $\chi_{i+1} = -20$ or 160° and the cross-hatched area to $0, 20$, or -160° . A difference of about 1.3 kcal mol⁻¹ in the energy between the conformation with $(\chi_{i-1}, \chi_{i+1}) = (20^\circ, 20^\circ)$ and $(20^\circ, -20^\circ)$ is due to the $(\text{CH}_3)_{i-1}$ – $\text{O}^{\text{C}}_{i+1}$ interaction distance.²⁴ In the former, it is 3.39 Å, and it reduces to 2.76 Å for $(20^\circ, -20^\circ)$.

The conformation of one of the skeletal bonds being at $\pm 73^\circ$ in the 5(2.08) helix emphasizes the importance of including the side group conformation as a variable in the energy calculations. Figure 9 shows the energy map for the meso dyad of PMMA, as a function of ϕ_i and ϕ_{i+1} . Values of 109.5 and 125° have been used here for θ' and θ'' , respectively. Contours are drawn at intervals of energy indicated in the figure, with respect to the minimum marked. The positions of the right-handed 5(2.08) helix are marked. In Figure 9a, which corresponds to $\chi_{i-1} = \chi_{i+1} = 0^\circ$, these positions are far removed from the minimum energy positions for the *tt*, *gt*, and *t \bar{g}* states. However, as shown in Figure 9b, if the values of χ_{i-1} and χ_{i+1} are shifted to -40° , a new minimum appears at $(\phi_i, \phi_{i+1}) = (-5^\circ, -75^\circ)$, and this is close to the 5(2.08) helical conformation. The energy of this minimum is about 2.76 kcal mol⁻¹ higher

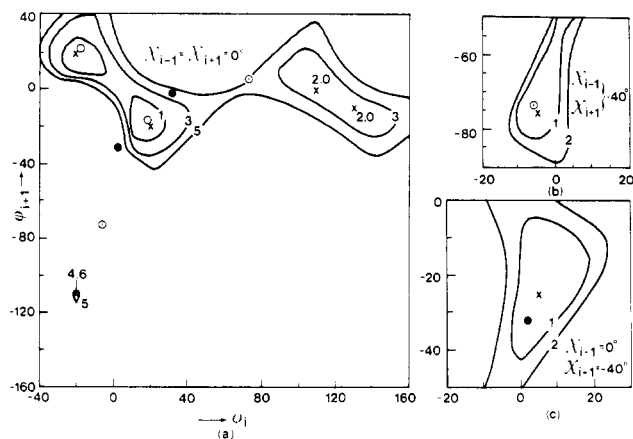


Figure 9. Energy contours for a meso dyad of PMMA in terms of ϕ_i and ϕ_{i+1} are shown. The side group rotations $\chi_{i-1} = \chi_{i+1} = 0^\circ$ in (a). Restricted regions of the map for side group rotations indicated therein are shown in (b) and (c). The values of E_0 corresponding to the minima in (a), (b), and (c) are -1.54 , 1.22 , and -1.16 kcal mol $^{-1}$, respectively. The positions of the 5(2.08) helix (\odot) and the 10(2.08) helix (\bullet) are marked.

than the minimum energy in Figure 9a. A shift of -40° in χ_{i-1} and χ_{i+1} is required to generate the minimum in the (ϕ_i, ϕ_{i+1}) surface shown in Figure 9b. Thus, χ_{i-1} and χ_{i+1} should be treated as variables so as to minimize the energy at each of the ϕ_i, ϕ_{i+1} conformations while constructing the energy diagram.²² Such an effort for the entire (ϕ_i, ϕ_{i+1}) surface is not made here, but it will be discussed for PMMA elsewhere.

Ten-Residue Helix. The results of the virtual bond analysis of the right-handed 10(2.08) helix are shown in Figure 10. The range of θ between 180 and 360° is shown here. It is seen that the value of θ'' varies from 114 to 131.6° in the range of θ shown here. The values of ϕ_i remain positive, and those of ϕ_{i+1} remain negative. For each of the values of θ'' , except at the maximum of the θ'' curve, two right-handed helices are possible. For example, for $\theta'' = 125^\circ$, right-handed 10(2.08) helices are possible with $(\phi_i, \phi_{i+1}) = (2^\circ, -32^\circ)$ and $(32^\circ, -2^\circ)$. Here, the conformation of one of the skeletal bonds is close to the perfect trans conformation, whereas the other is shifted by $\pm 32^\circ$. As the value of θ'' is increased, the values of ϕ_i and ϕ_{i+1} approach each other in magnitude, and at $\theta'' = 131.7^\circ$, a unique conformation with $(\phi_i, \phi_{i+1}) = (16.4^\circ, -16.4^\circ)$ results.

The energy curves are given in the upper part of Figure 10. For $\chi_{i-1} = \chi_{i+1} = 0^\circ$, two minima occur, at $\theta = 240$ and 305° , the former being of slightly lower energy. When $\theta = 240^\circ$, the value of θ'' is 128.3° and $(\phi_i, \phi_{i+1}) = (5.3^\circ, -27.9^\circ)$; for $\theta = 305^\circ$, these parameters are 127.1° and $(29.4^\circ, -4^\circ)$, respectively. These large values obtained for θ'' are similar to those used previously for the energy calculations on PMMA. Here too, the minimum at $\theta = 240^\circ$ is more sensitive to the variations in χ_{i-1} and χ_{i+1} than the minimum at $\theta = 305^\circ$. With $(\chi_{i-1}, \chi_{i+1}) = (20^\circ, 20^\circ)$, the energy at $\theta = 240^\circ$ is very high, due to severe steric interactions of the type $C_{i-1}^\beta - O_{i+1}^e$ (2 Å), $O_{i-1}^e - O_{i+1}^e$ (1.9 Å), and $O_{i-1}^e - (CH_3)_{i+1}^*$ (2 Å), and the minimum has vanished. However, when χ_{i+1} is assigned 0, -20 , or 160° , such interactions are relieved, and the energy decreases. It is also seen that the location of the minimum varies between $\theta = 220$ and 245° , depending on the values of χ , whereas the minimum at $\theta = 305^\circ$ is hardly affected. With $(\chi_{i-1}, \chi_{i+1}) = (160^\circ, -20^\circ)$, the energy of the minimum at $\theta = 230^\circ$ is lower by about 3.3 kcal mol $^{-1}$ than the minimum at $\theta = 305^\circ$.

The locations of the 10(2.08) helix on the (ϕ_i, ϕ_{i+1}) map, with $\theta'' = 125^\circ$, are shown in Figure 9. In this case also,

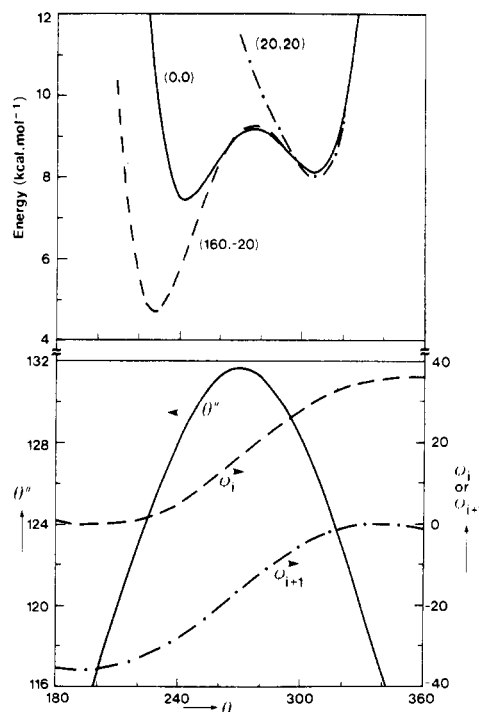


Figure 10. Results of the virtual bond analysis for the right-handed 10(2.08) helix of isotactic PMMA. See legend to Figure 3. The energy contours for three sets of side group rotation angles are shown in the upper part.

if $(\chi_{i-1}, \chi_{i+1}) = (0, 0^\circ)$, the positions of the helices with $(\phi_i, \phi_{i+1}) = (2^\circ, -32^\circ)$ and $(32^\circ, -2^\circ)$ are far removed from the minimum energy position for the tt state. However, as shown in Figure 9c, with $(\chi_{i-1}, \chi_{i+1}) = (0^\circ, -40^\circ)$, the minimum in the tt state shifts to $(\phi_i, \phi_{i+1}) = (5^\circ, -25^\circ)$. This minimum is very close to the 10(2.08) helix conformation with $(\phi_i, \phi_{i+1}) = (2^\circ, -32^\circ)$. Figures 9b and 9c also show that the energy of the 10(2.08) conformation is lower than that of the 5(2.08) conformation.

Conclusions

The application of the virtual bond method of analysis to study the crystalline conformations of vinyl chains has been demonstrated here. The analysis is simple and allows the energy minimization of the helical conformation with respect to the side group rotations and the skeletal bond angle $C^\beta - CH_2 - C^\alpha$. The positional coordinates of the atoms in the preferred helical conformation are available immediately and are useful for further structure analysis. Although it does not have the same convenience of demonstration with models as the rotations about the skeletal bonds, it is a simple mathematical method to analyze the helical conformation.

The stereochemical feasibility of the 12(2.55) helix for isotactic polystyrene and the fact that its energy is lower than that of the 3(2.216) helix deserve further analysis in terms of refinement of the respective structures and understanding of the conformational transition from one type to the other. The occurrence of the 3(2.216) helix under normal conditions implies the role of intermolecular as well as solvent-polymer interactions in the stabilization of the 12(2.55) helical structure. The existence of two types of structures for isotactic polystyrene has been indicated from studies on benzoylated polystyrene as well.²⁵ Rigorous attempts at comparing or refining the stereochemically derived 12(2.55) helix with X-ray data are not attempted here. The presence of head-to-head sequences in isotactic polystyrene, although in low concentration, has

been detected by Benson et al.²⁶ on the basis of a new resonance in the ¹³C NMR spectra. How far the presence of such head-to-head sequences influences the crystalline areas is unknown. The fact that the extended conformation in the gel reverts to the familiar 3(2.216) helical structure upon heating rules out the possibility of a significant proportion of head-to-head/tail-to-tail sequences in the polymer.

The crystalline conformation of isotactic PMMA is still a matter of debate.^{18,27} The virtual bond analysis shows that the isolated 5(2.08) helix is of higher energy than the 10(2.08) helix. It is likely that the conformational transition at 43° which Liquori and co-workers¹⁸ detected on the basis of ultraviolet spectra of PMMA corresponds to a transition between the 5(2.08) and the 10(2.08) helices. The former occurs close to a new minimum at $(\phi_i, \phi_{i+1}) = (-5, -75^\circ)$, generated by suitable adjustment of side group positions. In both cases, the rotations of the side groups are important variables in the choice of the preferred conformation and in assessing the relative positions of these helical structures in the overall (ϕ_i, ϕ_{i+1}) domain of the polymer.

Acknowledgment. The author is grateful to Dr. M. L. Hair and Dr. R. H. Marchessault of this research center for their interest in this work.

References and Notes

- (1) P. DeSantis, E. Giglio, A. M. Liquori, and A. Ripamonti, *J. Polym. Sci., Part A*, **1**, 1383 (1963).
- (2) P. J. Flory, "Statistical Mechanics of Chain Molecules", Interscience, New York, 1969.
- (3) A. Abe, R. L. Jernigan, and P. J. Flory, *J. Am. Chem. Soc.*, **88**, 631 (1966).
- (4) P. R. Sundararajan and P. J. Flory, *J. Am. Chem. Soc.*, **96**, 5025 (1974).
- (5) D. Y. Yoon, P. R. Sundararajan, and P. J. Flory, *Macromolecules*, **8**, 776 (1975).
- (6) D. Y. Yoon, U. W. Suter, P. R. Sundararajan, and P. J. Flory, *Macromolecules*, **8**, 784 (1975).
- (7) P. R. Sundararajan, *Macromolecules*, **10**, 623 (1977).
- (8) P. R. Sundararajan, *Macromolecules*, **11**, 256 (1978).
- (9) E. Benedetti, C. Pedone, and G. Allegra, *Macromolecules*, **3**, 16, 727 (1970).
- (10) R. H. Marchessault and P. R. Sundararajan, *Pure Appl. Chem.*, **42**, 399 (1975).
- (11) P. R. Sundararajan and R. H. Marchessault, *Can. J. Chem.*, **53**, 3563 (1975).
- (12) P. R. Sundararajan, R. H. Marchessault, G. J. Quigley, and A. Sarko, *J. Am. Chem. Soc.*, **95**, 2001 (1973).
- (13) P. R. Sundararajan in "Biomolecular Structure, Conformation, Function and Evolution", R. Srinivasan, Ed., Pergamon Press, London, in press.
- (14) A. D. French and V. G. Murphy, *Am. Chem. Soc. Symp. Ser.*, **48**, 42 (1977).
- (15) G. Natta, P. Corradini, and I. W. Bassi, *Nuovo Cimento, Suppl.*, **1**, 15, 68 (1960).
- (16) E. D. T. Atkins, D. H. Isaac, A. Keller, and K. Miyasaka, *J. Polym. Sci., Polym. Phys. Ed.*, **15**, 211 (1977).
- (17) C. W. Bunn, *Proc. R. Soc. London, Ser. A*, **180**, 67 (1942).
- (18) M. D'Alagni, P. DeSantis, A. M. Liquori, and M. Savino, *J. Polym. Sci., Part B*, **2**, 925 (1964); A. M. Liquori, Q. Anzuno, V. M. Coiro, M. D'Alagni, P. DeSantis, and M. Savino, *Nature (London)*, **206**, 358 (1965); V. M. Coiro, P. DeSantis, A. M. Liquori, and L. Mazzarella, *J. Polym. Sci., Part C*, **16**, 4591 (1969).
- (19) H. Kusanagi, H. Tadokoro, and Y. Chatani, *Macromolecules*, **9**, 531 (1976).
- (20) In this notation, $n(\pm h)$ denotes a helix with n residues per turn and an advance per monomer of h . The negative sign applies if the helix is left handed.
- (21) P. J. Flory, P. R. Sundararajan, and L. C. DeBolt, *J. Am. Chem. Soc.*, **96**, 5015 (1974).
- (22) U. W. Suter and P. J. Flory, *Macromolecules*, **8**, 765 (1975).
- (23) S. Havriliak and N. Roman, *Polymer*, **7**, 387 (1966); B. Schneider, J. Stokr, S. Dirlikov, and M. Mihailov, *Macromolecules*, **4**, 715 (1971).
- (24) The labels O^c and O^e denote the carbonyl and ester oxygen atoms, respectively. An asterisk is attached to the CH₃ of the (COOCH₃) group to distinguish it from the methyl group attached to the C^a atom.
- (25) N. Overbergh and H. Berghmans, *Polymer*, **18**, 883 (1977).
- (26) R. Benson, J. Maxfield, D. E. Axelson, and L. Mandelkern, *J. Polym. Sci., Polym. Phys. Ed.*, **16**, 1583 (1978).
- (27) V. M. Coiro, A. M. Liquori, P. DeSantis, and L. Mazzarella, *J. Polym. Sci., Polym. Lett. Ed.*, **16**, 33 (1978).

Stopped-Flow Study of the Cationic Polymerization of Styrene Derivatives. 4.^{1,2} Polymerization of *p*-Methoxystyrene by Superacid Initiators

Mitsuo Sawamoto and Toshinobu Higashimura*

Department of Polymer Chemistry, Faculty of Engineering, Kyoto University, Kyoto 606, Japan. Received December 20, 1978

ABSTRACT: Stopped-flow/rapid-scanning spectroscopy was applied to the cationic polymerization of *p*-methoxystyrene by superacid initiators (CF₃SO₃H and CH₃COClO₄) to afford absorption spectra of the propagating species centered at ca. 380 nm in (CH₂Cl)₂ at 30 °C. The absorbance at 380 nm rapidly increased, reached a maximum within 20–40 ms, and decayed gradually. Correspondingly, the monomer ([M]₀ = 5.0 × 10⁻³ M) was consumed in a millisecond time scale. From these data, rate constants of propagation (k_p) and initiation (k_i) were determined. The k_p values, ranging from 5.4 × 10⁴ to 1.3 × 10⁵ M⁻¹ s⁻¹, clearly exceeded those for other cationic initiators (I₂, BF₃O(C₂H₅)₂, etc.). The k_i values and initiation efficiency were much more dependent on initiators and in the order: CH₃COClO₄ ≥ CF₃SO₃H >> SnCl₄ ~ BF₃O(C₂H₅)₂ >> CH₃SO₃H > I₂. Thus, an important characteristic of the superacid initiators is to generate reactive propagating species very rapidly and efficiently. Polymerizations in (CH₂Cl)₂/CCl₄ mixtures or in (CH₂Cl)₂ containing a common ion salt also gave absorption spectra with the 380-nm peak but resulted in an unexpected increase in k_p based on this band. Involvement of an "invisible" propagating species that participates in monomer consumption without showing any absorption at λ > 300 nm was proposed and discussed.

The previous papers^{1,3,4} of this series deal with application of stopped-flow spectroscopy to the cationic polymerization of *p*-methoxystyrene by a variety of initiators. We have shown that the propagating species exhibits a

distinct absorption centered at ca. 380 nm in 1,2-dichloroethane ((CH₂Cl)₂)³ and have successfully determined rate constants of propagation (k_p)³ and initiation (k_i)¹ as well as the lifetime of the intermediate.¹ In spite of a minor